Bendre et al., https://doi.org/10.1083/jcb.201606081

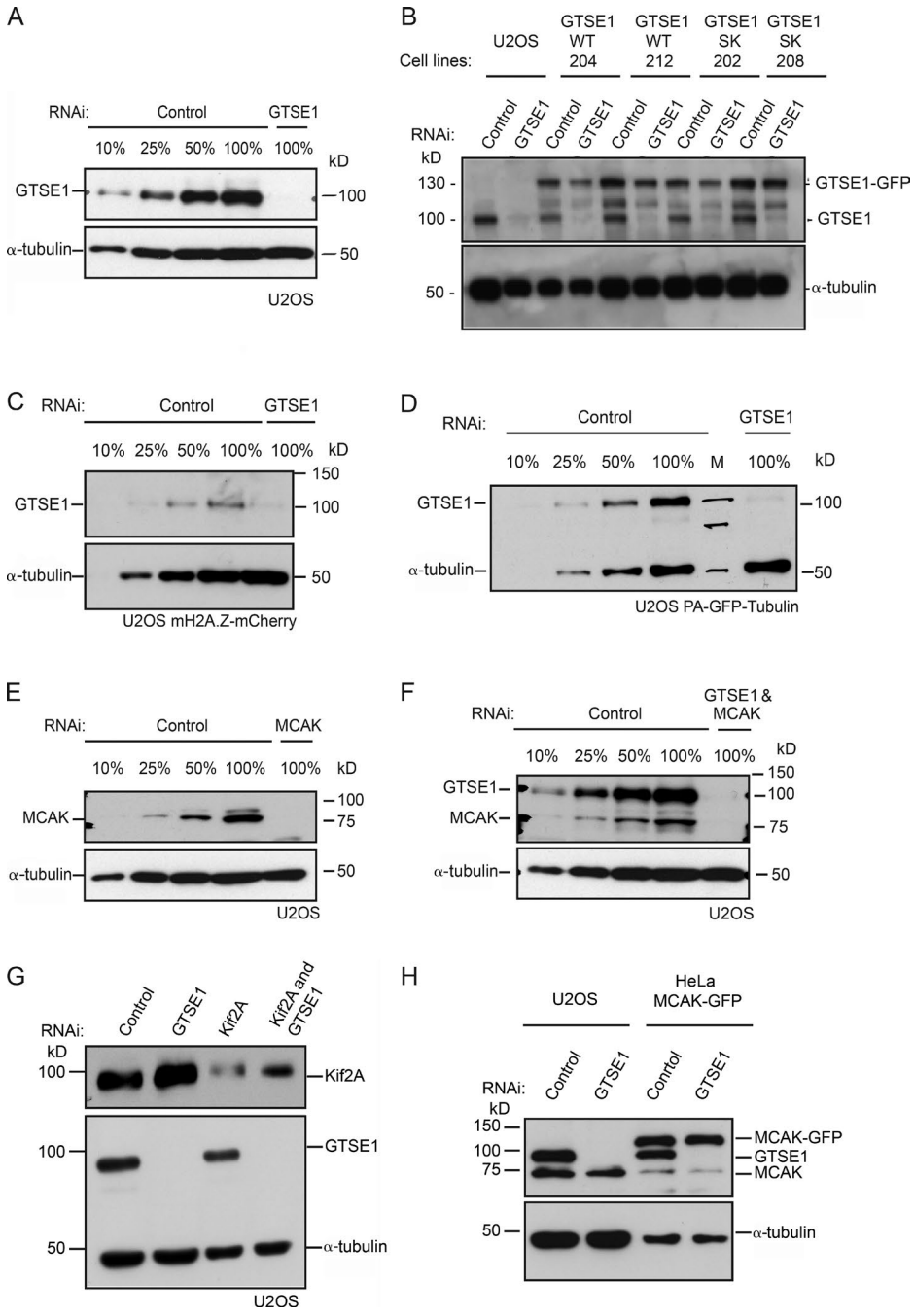

Figure S1. **Western blots showing RNAi depletion efficiency for all siRNAs and cell lines analyzed.** (A) Western blot of cell lysates after control (with dilutions indicated) or GTSE1 RNAi in U2OS cells, probed with anti-GTSE1 and anti–α-tubulin. GTSE1 levels are depleted to <10%. (B) Western blot of cell lysates after control or GTSE1 RNAi in U2OS cells, two stable U2OS cell clones expressing RNAi-resistant GTSE1 ($GTSE1^{WT(204)}$ and $GTSE1^{WT(212)}$), and two stable U2OS cell clones expressing RNAi-resistant GTSE1 mutated to abolish interaction with EB1 ($GTSE1^{Sk(202)}$ and $GTSE1^{Sk(208)}$). Blots were probed with anti-GTSE1 and anti–α-tubulin. (C) Western blot of cell lysates after control (with dilutions indicated) or GTSE1 RNAi in U2OS H2A.Z-mCherry cells, probed with anti-GTSE1 and anti–α-tubulin. GTSE1 levels are depleted to <25%. (D) Western blot of cell lysates after control (with dilutions indicated) or GTSE1 RNAi in U2OS PA-GFP-tubulin cells, probed with anti-GTSE1 and anti–α-tubulin. GTSE1 levels are depleted to <20%. M, positions of molecular weight markers. (E) Western blot of cell lysates after control (with dilutions indicated) or MCAK RNAi in U2OS cells, probed with anti-MCAK and anti–α-tubulin. MCAK levels are depleted to <20%. (F) Western blot of cell lysates after control (with dilutions indicated) or GTSE1 and MCAK RNAi in U2OS cells, probed with anti-GTSE1, anti-MCAK, and anti–α-tubulin. GTSE1 and MCAK levels are both depleted to <10%. (G) Western blot of cell lysates after control, GTSE1, Kif2A RNAi, and co-depletion of Kif2A and GTSE1 in U2OS cells, probed with anti-GTSE1, anti-Kif2A, and anti–α-tubulin antibodies. (H) Western blot of cell lysates after control or GTSE1 RNAi in U2OS cells and HeLa cells expressing BAC-based hKif2C-LAP, probed with anti-GTSE1, anti-MCAK, and anti–α-tubulin antibodies.

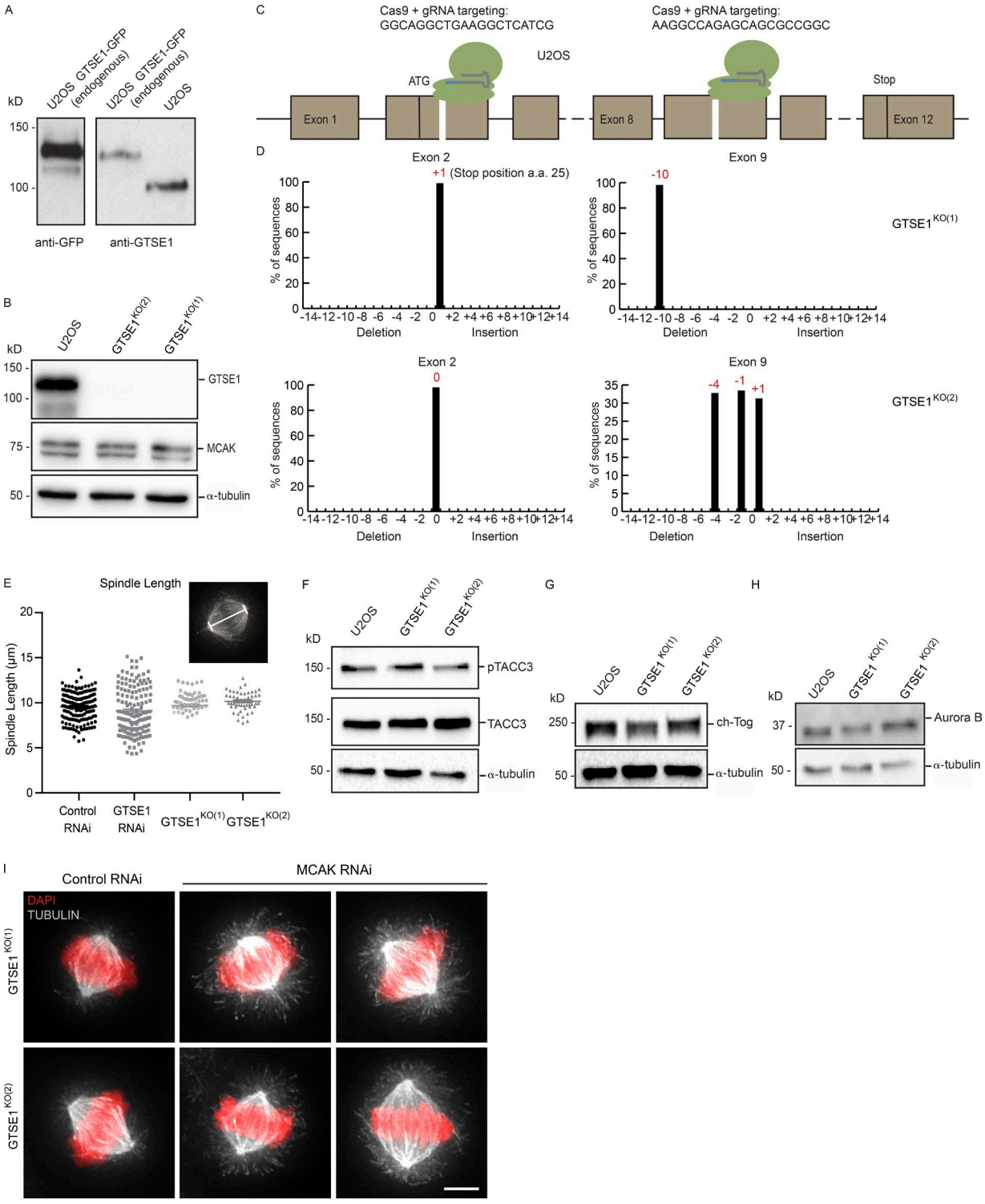

Figure S2. **Verification and characterization of Cas9 nuclease–mediated GTSE1-GFP and GTSE1 knockout clones.** (A) Western blots showing U2OS cells with endogenous GTSE1 protein tagged with GFP via Cas9-mediated homologous recombination. (B) Western blot of cell lysates from U2OS cells and two Cas9-mediated GTSE1 knockout U2OS clones run by SDS-PAGE and probed with antibodies against GTSE1, MCAK, and α-tubulin. (C) Scheme representing the GTSE1 locus and the two chosen sites targeted by the Cas9 nuclease for knockouts. The sequence targeted by each Cas9/guide RNA (gRNA) pair is indicated. (D) Regions surrounding the CRISPR-Cas9 cutting sites were amplified by PCR from genomic DNA and sequenced, and heterozygous insertions and deletions were resolved using TIDE software. Histograms show the percentage of sequences showing no modification ($n = 0$), an insertion ($n > 0$), or a deletion of n nucleotides ($n < 0$) at the CRISPR-Cas9 cutting site in exons 2 and 9 of the GTSE1 locus. Clones were generated by transfecting U2OS cells with a Cas9 nuclease targeting both exons 2 and 9 (clone 1) or exon 9 alone (clone 2). (E) Quantification of spindle length in U2OS cells after control and GTSE1 RNAi ($n \geq 145$ cells per condition; 4 independent experiments) and U2OS GTSE1$^{KO(1)}$ and GTSE1$^{KO(2)}$ cell lines ($n \geq 50$ cells each). The inset shows the region measured to obtain spindle length. (F–H) Western blot of cell lysates from U2OS cells and two Cas9-mediated GTSE1 knockout U2OS clones run by SDS-PAGE and probed with antibodies against pS558-TACC3, TACC3, ch-Tog, Aurora B, and α-tubulin. (I) Immunofluorescence images of mitotic GTSE1 knockout clones after control and MCAK RNAi, stained for DNA (DAPI) and MTs (tubulin). Bar, 5 μm.

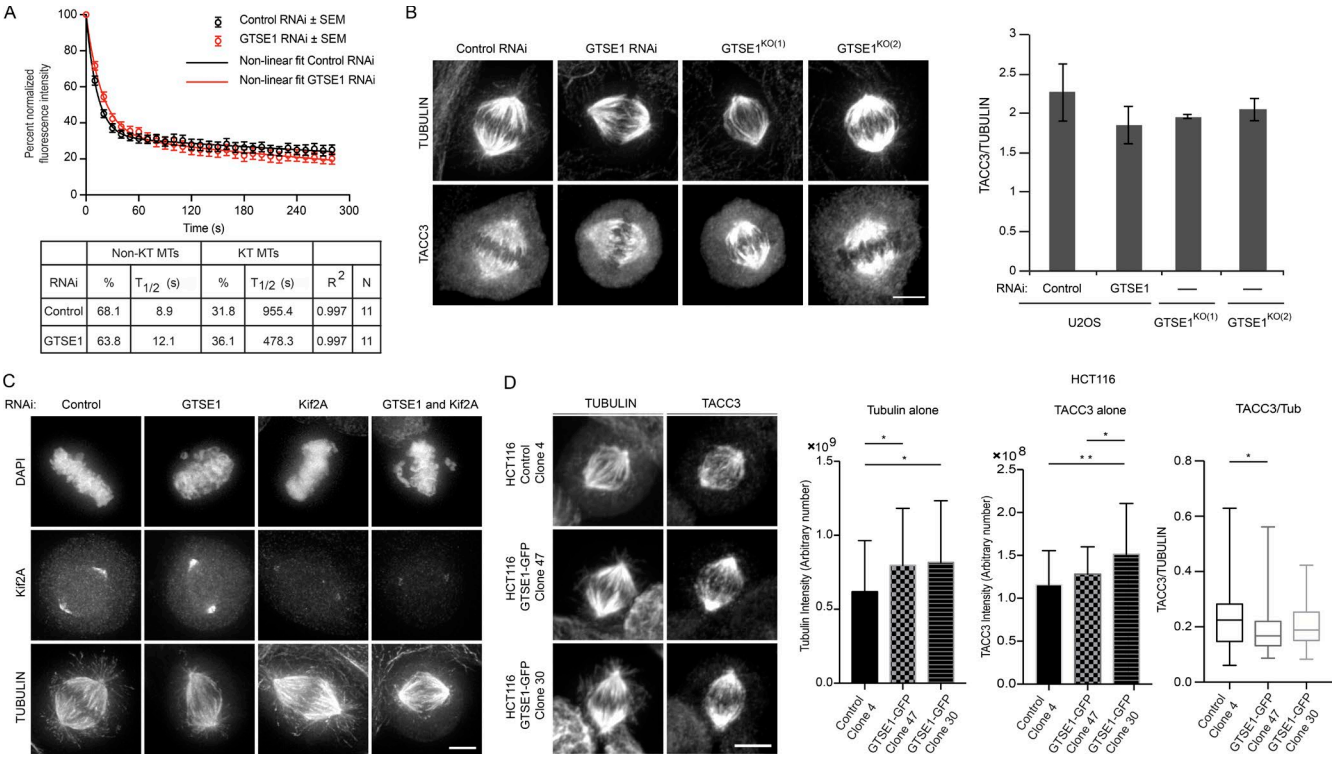

	Non-KT MTs		KT MTs			
RNAi	%	$T_{1/2}$ (s)	%	$T_{1/2}$ (s)	R^2	N
Control	68.1	8.9	31.8	955.4	0.997	11
GTSE1	63.8	12.1	36.1	478.3	0.997	11

Figure S3. **Analysis of kinetochore–MT stability, TACC3 localization, and Kif2A dependence after perturbation of GTSE1 expression.** (A) Graph showing mean normalized fluorescence intensity at each time point after photoactivation of PA-GFP-tubulin in U2OS metaphase spindles treated with control or GTSE1 RNAi. n = 11 cells per condition; over 3 independent experiments. Solid lines represent the double exponential fit for control and GTSE1 RNAi. KT, kinetochore. Error bars represent SEM. (B) Immunofluorescence images of mitotic U2OS cells after control and GTSE1 RNAi and stable GTSE1 knockout clones, stained for MTs (tubulin) and TACC3. The graph represents quantification of TACC3 on the mitotic spindle in U2OS cells after control or GTSE1 RNAi ($n \geq 50$ cells per condition; 3 independent experiments) and in stable GTSE1 knockout clones ($n \geq 50$ cells each; 2 independent experiments). Error bars represent SEM. Differences were not statistically significant. (C) Immunofluorescence images of mitotic U2OS cells after control, GTSE1, Kif2A, or combined GTSE1 and Kif2A RNAi, stained for DNA (DAPI), Kif2A, and MTs (tubulin). (D) Immunofluorescence images of mitotic HCT116 control and GTSE1-GFP–overexpressing clones stained for MTs (tubulin) and TACC3. The left graph represents mean tubulin fluorescence of the inner spindle from immunofluorescence analysis of HCT116 control and GTSE1-GFP–overexpressing clones. The middle graph shows mean TACC3 intensity of the inner spindle quantified from immunofluorescence analysis of HCT116 control and GTSE1-GFP–overexpressing clones. The right graph represents mean TACC3 intensity on the inner spindle normalized to tubulin intensity for HCT116 control and GTSE1-GFP–overexpressing clones. $n \geq 52$ cells per condition; 1 experiment. P-values were obtained using an analysis of variance and Tukey's test. Bars, 5 µm. Error bars represent standard deviation. *, $P \leq 0.05$; **, $P \leq 0.01$.

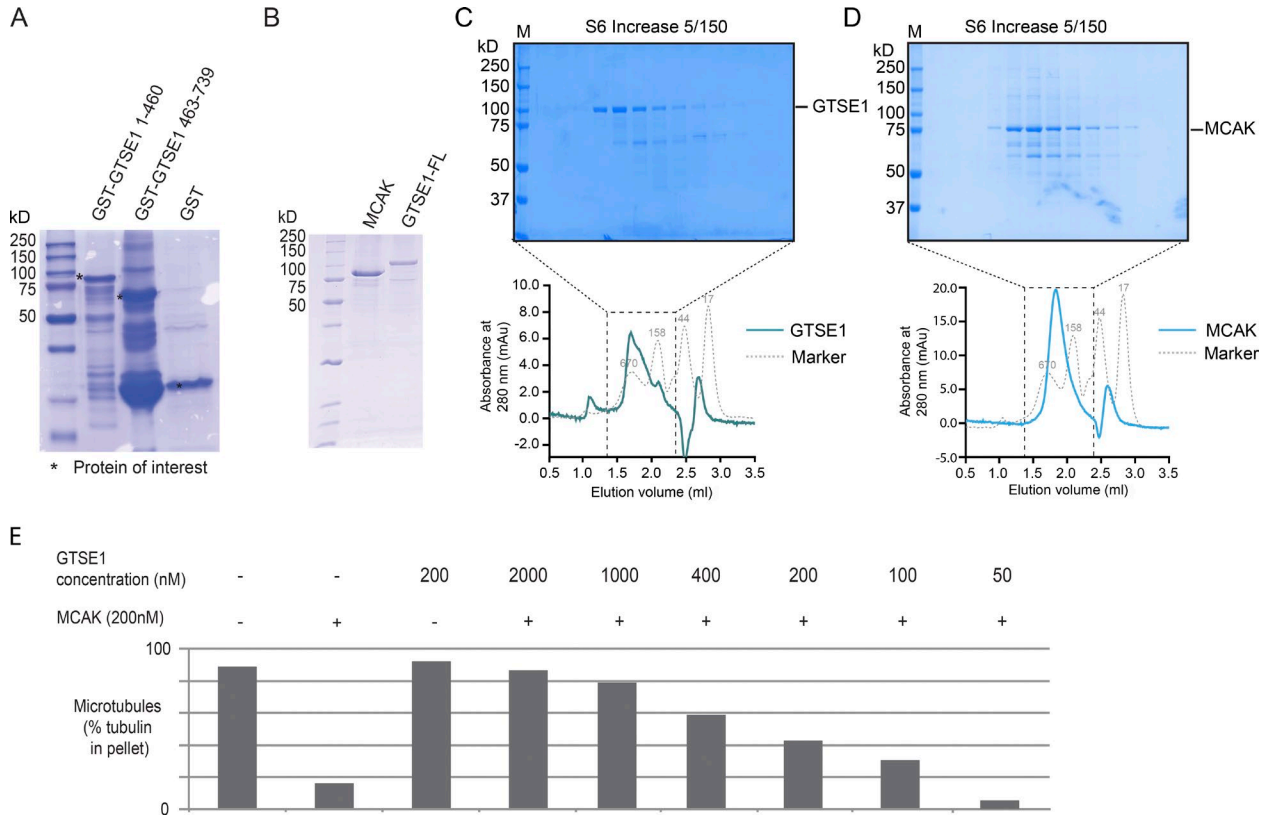

Figure S4. **In vitro analysis of GTSE1 inhibition of MCAK.** (A) Coomassie-stained SDS-PAGE gels of inputs from in vitro GST pulldown assays. (B) Gel showing full-length MCAK and GTSE1 purified from baculovirus-infected insect cells. Molecular weights are indicated to the left. (C) Size exclusion chromatography profile of full-length GTSE1 (78.5 kD) shows that the protein elutes earlier than expected, consistent with an elongated unfolded structure. (D) The size exclusion chromatography profile of full-length MCAK shows that MCAK (81 kD) runs as a dimer. M, molecular weight marker; mAu, milli absorption units. (E) In vitro sedimentation assay to monitor inhibition of MCAK depolymerase activity by GTSE1. Taxol-stabilized MTs were added to 200 nM MCAK and varying concentrations of GTSE1 in the presence of ATP. The reaction mixture was incubated for 1 h at room temperature followed by centrifugation at high speed. Supernatants and pellets were collected, and equal amounts were run on SDS-PAGE gel and stained with Coomassie blue. The histogram shows the percentage of tubulin for each condition in the pellet fraction, quantified from the density of the Coomassie gel from a representative experiment.

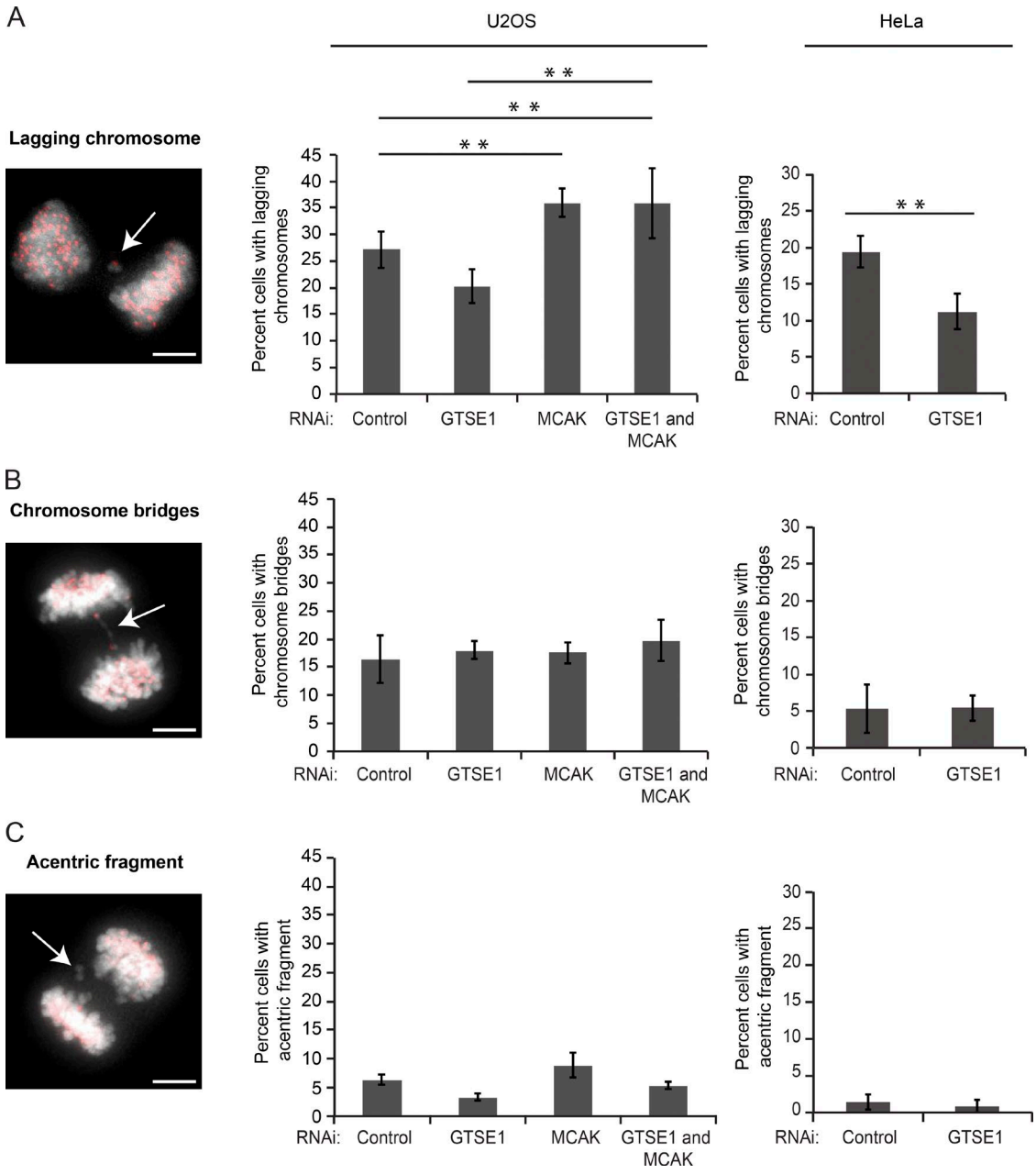

Figure S5. **Quantification of anaphase chromosome segregation defects in U2OS and HeLa cells after GTSE1 and/or MCAK RNAi depletion.** (A) Quantification of anaphase-lagging chromosomes. The white arrow indicates a lagging chromosome. (B) Quantification of chromosome bridges. The white arrow indicates a chromosome bridge. (C) Quantification of acentric fragments. Error bars represent SEM. The white arrow indicates an acentric fragment. *n* > 220 U2OS cells with defective anaphases; 3 independent experiments. *n* > 390 HeLa cells with defective anaphases; 3 independent experiments. Bars, 5 µm. **, P ≤ 0.01.

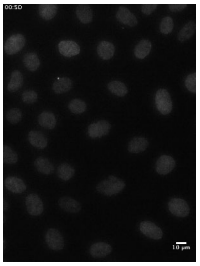

Video 1. **Chromosome dynamics and mitotic progression in control U2OS cells.** Mitotic cells efficiently align chromosomes and enter anaphase. U2OS histone H2A.Z-mCherry cells after control RNAi were imaged at 1-min intervals and are displayed at eight frames per second.

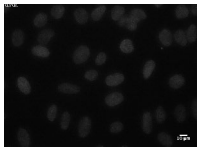

Video 2. **Chromosome dynamics and mitotic progression in GTSE1-depleted U2OS cells.** Mitotic cells have difficulty aligning chromosomes and delayed mitotic timing, yet are able to eventually align chromosomes and enter anaphase. U2OS histone H2A.Z-mCherry cells after GTSE1 RNAi were imaged at 1-min intervals, and the video is displayed at eight frames per second.

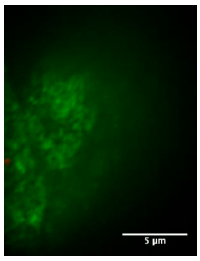

Video 3. **GTSE1 localization to kinetochore MTs.** Representative z stack of a U2OS cell showing GTSE1 localization to kinetochore MTs. The U2OS cells were treated with cold for 17 min and then stained for GTSE1 and CREST (kinetochore). The video is displayed at eight frames per second.

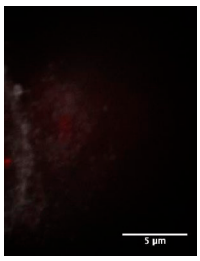

Video 4. **Kinetochore MTs in U2OS cells.** Representative z stack of a U2OS cell (same as in Video 3) showing MTs in gray (tubulin) and kinetochores (CREST) in red. The video is displayed at eight frames per second.

Video 5. **GMPCPP-stabilized MTs in the presence of 50 nM MCAK.** Epifluorescence images of GMPCPP-stabilized MTs were captured at 5-s intervals for 5 min. The GMPCPP-stabilized MTs were observed to depolymerize rapidly from both ends in the presence of 50-nM MCAK. Video playback is 45× real time (see time stamp).

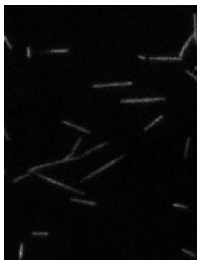

Video 6. **GMPCPP-stabilized MTs in the presence of 50 nM MCAK and 250 nM GTSE1.** Epifluorescence images of GMPCPP-stabilized MTs were captured at 5-s intervals for 5 min. The GMPCPP-stabilized MTs were observed to maintain a constant length in the presence of 50-nM MCAK and 250-nM GTSE1. Video playback is 45× real time (see time stamp).